Maximizing the surge amplitude of a floater through an adaptable mooring tightening technique

Andreas T. Asiikkis, Dimokratis G.E. Grigoriadis, and Antonis I. Vakis

Abstract— **A technique to maximize the surge amplitude of a floater using an adaptable mooring tightening technique is presented in this study. A series of numerical simulations and experiments were conducted to understand the effect of the mooring cable length and stiffness on the surge response under various sea states. WEC-Sim was employed to solve the multi-body dynamics of a rectangular cuboid floater whereas MoorDyn modelled the mooring dynamics using a lumped-mass formulation. Experiments in a small-scale wave tank validated the accuracy of the numerical model. The results indicated that the surge motion of the floater can be amplified when the mooring cables are tightened, but the heave mooring forces increase due to the higher cable tension. Moreover, both the heave amplitude and the mean floater position exhibit a downward trend when the length of the mooring decreases, implying a shift of the oscillatory motion from the vertical (heave) to the horizontal (surge) direction. However, overtightening the cables resulted in reduced surge motion and significantly increased mooring forces, potentially compromising the cables' integrity. The optimal cable length was identified for various stiffness values and sea states. These findings pave the way for designing new Wave Energy Converters (WECs) that exploit the surge motion of floaters instead of the conventional heave-focused approaches by adjusting the length of the mooring lines.**

Keywords—Adaptable mooring, MoorDyn, Multi-body dynamics, Surge Wave Energy Converter, WEC-Sim.

I. INTRODUCTION

A. Wave Energy Converters

WAVE energy converters (WECs) have emerged as a promising renewable energy solution in recent years, attracting considerable research attention due to the abundant wave energy resources available in the ocean, [1], [2]. Literature suggests that WECs can generate more than 4% of the available 2.1 TW global wave power resource [3] and more than 1000 designs exist for WEC technologies each based on distinct operating principles, [4].

One widely recognized design is the point absorber technology, which utilizes a floater to extract energy from its heave motion. Several notable examples of point absorber technologies can be found in the literature [5], [6]. In addition, there is the concept of the oscillating surge WEC [7], which extracts the horizontal motion of the waves. In the present study, we explore a new approach to maximize the surge motion of a floater connected to a mooring line which could be used as a point absorber WEC working primarily in the surge direction rather than heave.

B. Optimization techniques for WECs and moorings

Many researchers focused on enhancing the response of floaters and maximizing the generated power by utilizing optimization techniques through adjustments of the geometry [8] or the Power-Take-Off (PTO) system [9]. Alamian et al. (2019), demonstrated that by optimizing the geometry of a pitch point absorber WEC, it is possible to enhance power extraction efficiency while reducing production costs [10]. Shi et al. (2019), investigated how the mass and cross-sectional area can affect the motion of the floater [11] whereas Dang et al. (2019) proposed a PTO system which can be tuned to the frequency of the waves, imposing resonance and increasing the power extraction

Sponsor and financial support acknowledgement: This publication resulted from research supported and Co-Funded by the Multimarine Services Ltd and the CMMI – Cyprus Marine and Maritime Institute. CMMI was established by the CMMI/MaRITeC-X project as a "Center of Excellence in Marine and Maritime Research, Innovation and Technology Development" and has received funding from the European Union's Horizon 2020 research and innovation program under grant agreement No. 857586; and by a matching funding from the Government of the Republic of Cyprus.

A. T. Asiikkis: CMME, Engineering and Technology institute Groningen, University of Groningen, Groningen, Netherlands & UCY-CompSci, Mechanical & Manufacturing Engineering Department, University of Cyprus, Nicosia, Cyprus (e-mail: a.asiikkis@gmail.com).

D. G. E. Grigoriadis: UCY-CompSci, Mechanical & Manufacturing Engineering Department, University of Cyprus, Nicosia, Cyprus (e-mail: dimokratisg@gmail.com).

A. I. Vakis: CMME, Engineering and Technology institute Groningen, University of Groningen, Groningen, Netherlands (e-mail: a.vakis@rug.nl).

Digital Object Identifier: https://doi.org/10.36688/ewtec-2023-274

[12]. In summary, the literature provides evidence that the geometry and PTO systems of buoys can be tuned to enhance the motion of the system, yielding higher energy extraction.

The optimization of mooring lines in offshore engineering plays a significant role in the integrity and performance of floater-mooring systems as well. Usually, the selection of mooring line parameters such as pretension, diameter etc. for the design of moorings, relies mainly on manual approaches despite the existence of advanced modelling tools [13]. Ja'e et al. (2022) highlighted the importance of adopting an integrated riser-mooring design methodology and discuss various evolutionary algorithm techniques, such as differential evolution, variants of genetic algorithms and particle swarm optimisation [13]. Wilson et al. (2021) presented a linearized modelling and optimization procedure for shared mooring systems by testing different array layouts in order to maximize the efficiency of the mooring system [14]. A genetic algorithm-based optimization procedure was proposed by Ferri et al. (2022) to find the favourable configuration of a floating wind turbine-mooring system for reducing its dynamic response in the surge, heave and pitch directions [15]. Optimization techniques have proven to be valuable for enhancing the performance of mooring systems, ensuring their integrity and efficiency.

C. *Modelling tools*

Modelling tools play a crucial role in the process of designing and optimising the performance of mooring-floater systems such as WECs. They provide valuable means to simulate and analyse the complex hydrodynamic interactions between the structure and the surrounding environment. A variety of modelling tools are available for simulating WECs, each offering its own set of unique capabilities and limitations.

WEC-Sim, a time-domain WEC simulator, utilizes hydrodynamic coefficients retrieved from frequency domain Boundary Element Methods (BEM) and then solves the Cummins equation [16] in the time domain. It has been extensively used to predict the performance of WECs by several researchers [17] and is the main numerical tool used in the present work. It can be categorized as a mid-fidelity tool, offering a balance between accuracy and computational efficiency. In addition, higher-fidelity tools, such as Computational Fluid Dynamics (CFD) codes, are available, providing more detailed analysis of the interaction between the floating structures and water flow and allow the simulation of extreme conditions such as breaking waves. OpenFOAM is the most famous CFD code used for WEC simulations [18] with several examples in the literature [19], [20] whereas other codes are being used as well, including Ansys FLUENT [21], and Flow-3D [22].

D. *Study overview*

Herein, we investigate means of amplifying the surge motion of moored floaters for purposes of energy extraction. We developed a numerical model using WEC-Sim and MoorDyn, allowing us to study the performance of a floater under a variety of conditions. Our main interest lies in adjusting the unstretched length of taut mooring lines and understanding how this change affects the surge response of the floater. By running a series of simulations with different stiffness values and wave conditions, we aim to clarify the complex relationship between these parameters. This study offers important insights by providing a potential adjustment parameter, which is the unstretched length of the mooring lines, to enhance the surge motion of a floater, and opens up the possibility for more effective use of this motion in future WEC designs.

II. MODEL AND METHODOLOGY

E. *Numerical Model*

1) *WEC-Sim*

To solve for the multi-body dynamics of the floater, the open-source WEC-Sim (Wave Energy Converter Simulator) software was used, developed in MATLAB and Simulink. It solves the 6-Degrees Of Freedom (DOF) equation of motion of floating bodies for their power performance prediction and design optimization.

The hydrodynamic characteristics of the floating bodies are given as inputs from a frequency-domain Boundary Element Method (BEM) solver; in this case Capytaine was used, a Python-based linear potential flow BEM solver. The solutions rely on the assumptions that the flow is inviscid, incompressible and irrotational.

Using a time-domain formulation, WEC-Sim calculates the dynamic response of a floating body by solving the following equation of motion about the centre of gravity:

$$m\frac{d^2X}{dt^2} = F_{ex}(t) + F_{md}(t) + F_{rad}(t) + F_{pto}(t) + F_v(t) + F_{me}(t) + F_B(t) + F_m(t) \quad (1)$$

where, m denotes the mass matrix of the floating body, X is the translational and rotational displacement, and $F_{ex}(t)$ is the wave excitation force and torque. $F_{md}(t)$ refers to the mean drift force and torque vector, whereas $F_{rad}(t)$ stands for the force and torque vector arising from wave radiation. $F_{pto}(t)$ indicates the force and torque from the Power-Take-Off (PTO) system, and $F_v(t)$ corresponds to the damping force elements. $F_{me}(t)$ represents the Morison element, $F_B(t)$ is the net buoyancy restoring force and torque calculated based on the hydrostatic stiffness and the mass of the body, and $F_m(t)$ is the force and torque due to the mooring connection.

For the numerical model developed in this work, the force term $F_{pto}(t)$ for the PTO system is neglected since a PTO was not considered for the purpose of this study. Moreover, the floater in this study was constrained to 3

DOF, focusing on heave, surge and pitch motions as these modes of motion were the most dominant. It is also noted that the term $F_{md}(t)$ is excluded since WEC-Sim does not support mean drift coefficients from Capytaine. More information about the theoretical background of WEC-Sim can be found in [23].

2) Capytaine

The hydrodynamic coefficients provided by the Capytaine BEM are used for the calculation of the $F_{ex}(t)$, $F_{rad}(t)$ and $F_B(t)$ terms. The BEM also provides the added mass matrix $A(\omega)$ and the wave damping term $B(\omega)$, as functions of frequency, which are incorporated in the wave radiation term given by $F_{rad}(t) = -A(\omega)\ddot{X} - B(\omega)\dot{X}$. More information about the theoretical background of Capytaine can be found in [24].

3) MoorDyn

MoorDyn [25] is an open-source, lumped-mass mooring line model, coupled with WEC-Sim, developed with a focus on predicting the dynamics of typical mooring systems. The coupled code has been extensively validated through experiments [26]. MoorDyn can be also coupled to other software such as FAST v8 [27] or OpenFOAM [28]. It considers internal axial stiffness, damping forces, weight and buoyancy forces, as well as hydrodynamic forces based on Morison's equation. MoorDyn is built on a lumped-mass approach, discretizing the cable dynamics along the length of the mooring line into evenly sized segments, which connect node points. The ends of each mooring line are identified by connection objects, which can be categorized into a) fixed, b) vessel, and c) connect nodes. Fixed nodes are immovable and serve as anchor points, vessel nodes can move under the control of an external program and connect nodes can move according to the forces acting on them and are used to connect two or more mooring lines together. In the present work, only fixed and vessel connections were used to connect the mooring line to the seabed (fixed connection) and the floater (vessel connection).

F. Experimental set-up

4) Wave tank

The experiments were conducted at the custom wave tank of the CMME group of the University of Groningen in the Netherlands. A schematic representation of the experimental set-up is illustrated in fig. 1. The wave tank, with dimensions of 9.57 m in length, 0.77 m in width, and 1.2 m in height, was filled up with water to a level of 0.65 m. A flap wave generator (fig. 2c) was used to generate the waves whereas an absorbing beach (fig. 2b) with a foam layer material was used to minimize the reflections. A cuboid wooden floater (fig. 2a) was used as the floating body with dimensions of 0.20 $m \times 0.07\ m \times 0.14\ m$, resulting in a draft of 0.045 m and a mass of 1.26 Kg. The floater was suitably positioned in the wave tank, with further details illustrated in fig. 1. The mooring lines were made of nylon rope of 5 mm in diameter with a linear density of 0.00733 Kg/m.

5) Free surface elevation measurements

The free surface elevation of the water was recorded with an ultrasonic sensor. Placed at a distance of 1.25 m upstream of the floater from the direction of wave propagation, the sensor was recording the free surface elevation prior to the wave impacts on the floater. Despite its modest measurement resolution of 0.3 cm and a sampling rate of 40 Hz, the sensor effectively captured the wave elevation data without significant signal noise, validating its cost-effective selection. The recorded data were transferred to a computer for further analysis using a microcontroller, resulting an inexpensive yet efficient setup.

6) Floater response measurements

To capture the response of the floater in the heave, surge, and pitch DOFs, a two-marker setup was implemented. Two markers of red and blue colour were positioned on the top of the floater as shown in fig. 1, enabling tracking of their motion via an image processing technique presented in [29]. A high-resolution camera, equipped with a 24-bit colour depth per pixel, was utilized

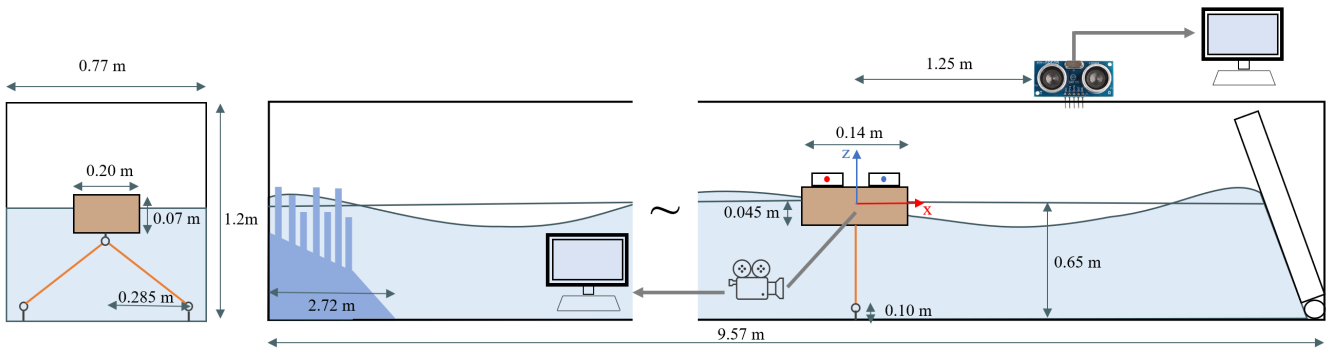

Fig. 1. Schematic of the experimental setup showing the dimensions of the wave tank, the cuboid floater and the mooring lines. The positioning of the camera and ultrasonic sensor is also shown. The wave tank features a flap wavemaker and an absorbing beach. The axes are not to scale.

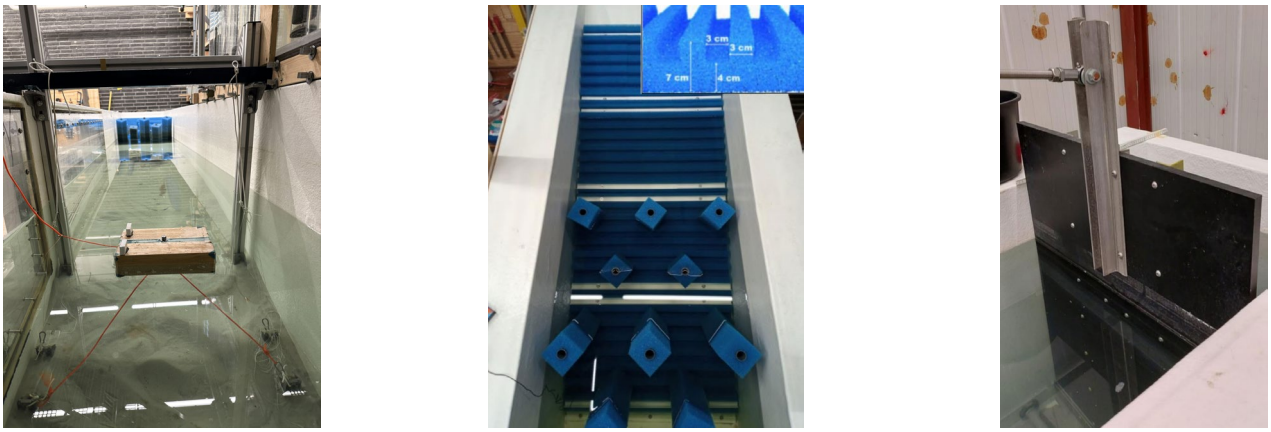

a) b) c)

Fig. 2. The experimental setup: a) floater connected to the seabed with mooring lines, b) absorbing beach with foam layer and foam pillars, c) the flap wave maker.

to record the position of the two markers at a rate of 30 frames per second, ensuring the accurate capture of the response. The tracking of the floater in the heave and surge directions was established by determining the coordinates of the centre of gravity based on the coordinates of the two markers over time. The pitch motion of the floater was accurately recorded by calculating the angular displacement of the line connecting the two markers, relative to the x-axis. This approach ensured complete capture of the floater's dynamic behaviour.

III. NUMERICAL SET-UP AND SENSITIVITY ANALYSIS

G. *Numerical model configuration*

In the numerical setup of this study, we utilised three primary tools to simulate the behaviour of the cuboid floater under different conditions. Firstly, Capytaine was used to obtain the hydrodynamic coefficients of the floater. A critical phase of this stage was conducting a comprehensive surface mesh sensitivity analysis to ensure the accuracy and reliability of the results. The optimum mesh configuration was chosen based on this analysis, providing a reliable foundation for our subsequent simulations in WEC-Sim.

Following the Capytaine simulations, we then utilized WEC-Sim and MoorDyn to simulate the dynamics of the floater and the mooring lines, respectively. The main numerical stability parameters of these tools include the time-step used in WEC-Sim, the time-step used in MoorDyn and the number of segments to discretise the mooring lines in MoorDyn. Several cases of different time-steps and mooring line segments were simulated to find the values which provide reliable results and at the same time keep the computational cost low. The combination of these software tools constitutes the foundation of our numerical setup and the sensitivity analyses performed ensures that the analysis of the floater's response under different wave and geometry conditions is trustworthy. In the following subsections, the analysis of the numerical stability and the validation of the numerical model with the experiments will be presented.

H. *Capytaine set-up and mesh sensitivity*

The resolution of the surface mesh in Capytaine can affect the results of the hydrodynamic response of the floater. To retrieve accurate results of the hydrodynamic coefficients from Capytaine, a fine mesh is needed. In table I the main input parameters to the BEM model are presented. The input parameters include the centre of gravity, range of wave frequencies, water depth, density and the geometrical configuration provided by facets of an .stl file. It is noted that the free surface of the water (i.e., waterline) is provided by specifying the xy plane at 0.01 m above the centre of gravity in the input geometry.

In fig. 3 the results of the normalized added mass $\bar{A}(\omega) = A(\omega)/\rho$ and radiation damping $\bar{B} = B(\omega)/\rho\omega$ are shown in the heave, surge, and pitch directions over a

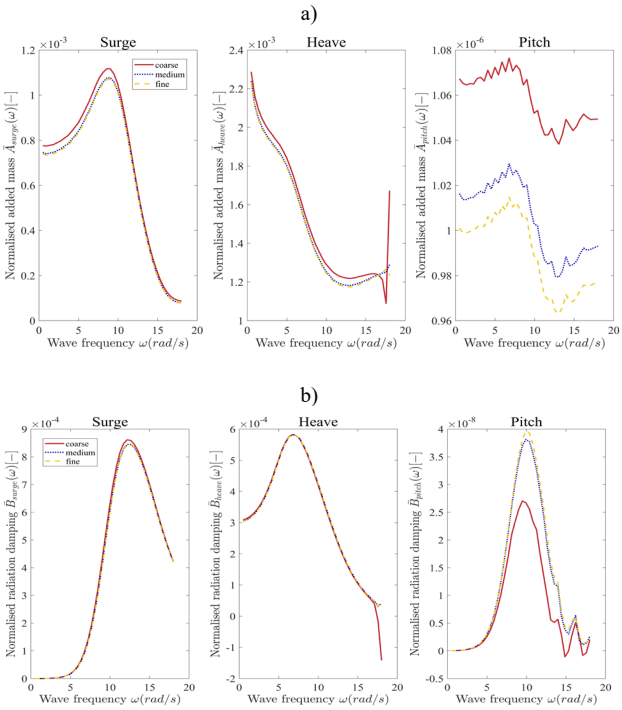

Fig. 3. a) Normalised added mass (top) and b) Normalised radiation damping (bottom) along the surge, heave and pitch directions over a spectrum of wave frequencies for 3 mesh sizes – coarse, medium and fine.

TABLE I
INPUT PARAMETERS TO THE CAPYTAINE BEM

Symbol	Input	Value
C_g	Centre of gravity	-0.01 m
ω	Wave frequencies	0.5-18 rad/s
$d\omega$	Frequency step	0.4375 rad/s
h	Water depth	0.65 m
ρ	Density of water	1025 Kg/m^3
N	Number of facets	176 (coarse)
		1440 (medium)
		8288 (fine)

Input parameters given for the Capytaine model to calculate the hydrodynamic coefficients of the floater.

range of wave frequencies and for three different mesh sizes (i.e., coarse, medium, fine). The results suggest that the fine mesh is converged, indicating that increasing the mesh density further would not significantly alter the results. To quantify the convergence study, the average relative difference between the results of the three mesh configurations is presented in table II. A lower relative difference between the medium and fine mesh, compared to the difference between the coarse and medium mesh, confirms the convergence. This verifies the effectiveness of the fine mesh in accurately calculating the hydrodynamic coefficients of the floater, making it the preferred choice for the subsequent simulations in WEC-Sim.

I. WEC-Sim and MoorDyn set-up and sensitivity analysis

In this section all the relevant information for setting up the simulations in WEC-Sim and MoorDyn is introduced. The response of the floater was simulated under regular waves with a wave height of $0.0506\,m$ and a period of $1.68\,s$ which are the wave conditions measured in the experiments. The floater's moment of inertia was set as 0.005, 0.003, and $0.006\,Kg\cdot m^2$ along the x, y, and z-axes, respectively. To simulate only the most dominant motions, the floater's degrees of freedom were constrained to heave, surge, and pitch. The total simulation time was 110 seconds with a ramp time set to 5 seconds which was the time needed to reach steady state wave-excitation forces.

MoorDyn was used to model the dynamics of the mooring lines and, as illustrated in fig. 1, two mooring lines were configured accordingly. Their stiffness was set to 2950 N, equivalent to that of nylon ropes, based on available literature [30]. It is noted that the definition of stiffness used here is based on the product of the Young's modulus E and the cross-sectional area A of the rope and was calculated using the following equation:

$$EA = 1.1810 \times 10^5 d^2 kN \qquad (2)$$

where d is the diameter of the rope. The rope's linear density and diameter were set to $0.00733\,Kg/m$ and $0.005\,m$ respectively.

To appropriately select the time-steps in the two codes and the number of mooring line segments, the test-cases presented in table III were simulated. Three different values for the number of mooring line segments n and three different values for the two time-steps, dt_{WS} and dt_{MD} for WEC-Sim and MoorDyn, respectively, were evaluated. The tension in the mooring lines over time is considered as the most important parameter of the sensitivity analysis in this work. This is because a taught mooring configuration is used and tensions can rise significantly under extreme wave conditions. Specifically, it is expected that the temporal variation of mooring tension should reach a consistent profile, characterized by consistent peaks, while the time-step is reduced and the number of mooring line segments increases. In fig. 4 the results of all the cases are summarised, showing the tension of the mooring lines over a small timeframe (zoom-in) where the tension variation has reached a steady state behaviour. From these results, the configuration with 25 mooring line segments is shown to provide a sufficiently converged solution, as revealed by the minimal differences observed between the three cases. Furthermore, the tension values appear to be unaffected by variations in the MoorDyn timestep, suggesting its negligible impact on the model's accuracy; hence, the timestep of $0.01\,ms$ was adopted. Lastly, the timestep of WEC-Sim showed a

TABLE II
RELATIVE PERCENTAGE DIFFERENCE BETWEEN MESHES

Added mass	Relative difference [%]		
Meshes	Surge	Heave	Pitch
Coarse-medium	4.72	3.19	5.02
Medium-fine	1.01	0.633	1.52
Radiation damping	Relative % difference		
Meshes	Surge	Heave	Pitch
Coarse-medium	3.56	5.78	49.2
Medium-fine	0.705	0.224	3.85

Relative percentage difference between the different mesh resolutions for the added mass and radiation damping and for the surge, heave and pitch motions.

TABLE III
TEST-CASES FOR SENSITIVITY ANALYSIS

Number of segments		
n	dt_{MD}	dt_{WS}
15	0.000005	0.00125
25	0.000005	0.00125
35	0.000005	0.00125
MoorDyn time-step		
n	dt_{MD}	dt_{WS}
25	**0.00001**	0.00125
25	0.000005	0.00125
25	0.0000025	0.00125
WEC-Sim time-step		
n	dt_{MD}	dt_{WS}
25	0.00001	0.0025
25	0.00001	**0.00125**
25	0.00001	0.000625

Test-cases used for the sensitivity analysis of the number of mooring line segments and time-steps used in MoorDyn and WEC-Sim. The bold values indicate those that were selected for the subsequent simulations.

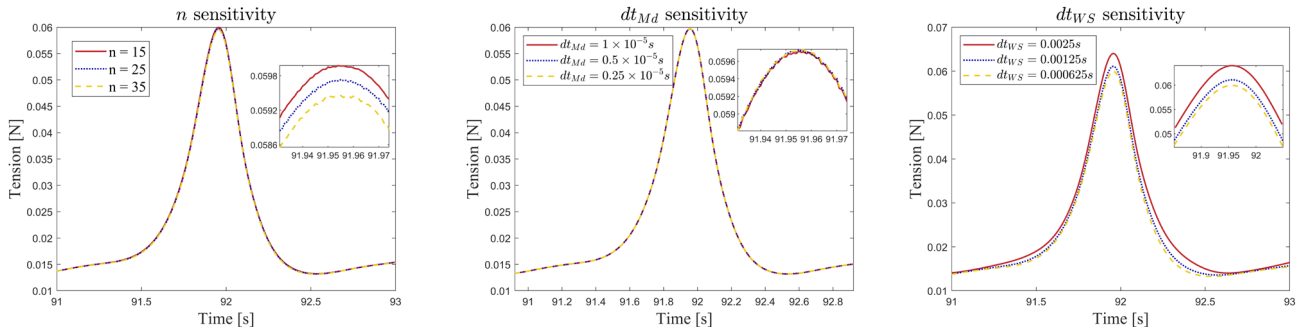

Fig. 4. Sensitivity analyses of a) the number of mooring line segments, b) MoorDyn time-step, and c) WEC-Sim time-step, as demonstrated by the tension in the mooring lines during the steady-state conditions.

tendency towards convergence at the value of 1.25 ms, establishing it as the optimal selection for the subsequent simulations.

IV. RESULTS AND DISCUSSION

J. *Model validation through experiments*

The present numerical model was tested against experiments to ensure its validity. This critical verification of the model involved the analysis of several parameters, including the wave conditions and the motion of the floater along the heave, surge and pitch directions. To showcase the most indicative data of our analysis, focus is made in the timeframe of 90-100 seconds. This decision is based on the observation that both the simulation and the experiments reached steady conditions after 80 seconds. This ensures that any transient effects from the initiation of the wave excitation forces, which are different in the simulations and the experiments, were diminished and the model settled to a regular pattern. Furthermore, it is noted that the timing of the numerical results was adjusted to align with the experimental measurements. This phase shift is essential due to the unavoidable discrepancy in the precise initiation of the experiments and the simulations, and allows for a more direct and fair comparison.

7) *Free-surface elevation*

In fig. 5, the free surface elevation measured by the ultrasonic sensor (dashed red line) at the upstream of the floater is compared to the wave input in WEC-Sim (solid blue line). The experimental signal exhibits some noise which is attributed to the resolution of the sensor. Nevertheless, the values of crests and troughs indicate repeatability with negligible differences, demonstrating the consistency of the measurements. Compared to the model's wave input, there is a close match, suggesting that the wave input of the numerical model matches with the waves encountered by the floater in the experiment.

8) *Response of the floater*

In fig. 6, the surge, heave and pitch responses of the floater over the timeframe of 90-100 seconds is presented. The surge and heave motions are captured with good

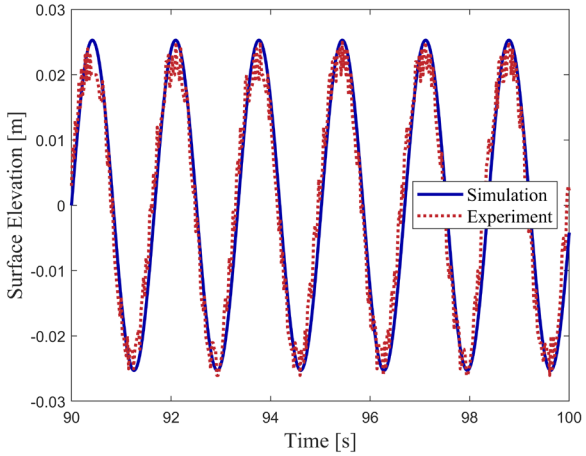

Fig. 5. Free surface elevation measurements from the experiments at 1.25 m upstream of the floater and wave input in the numerical model of WEC-Sim

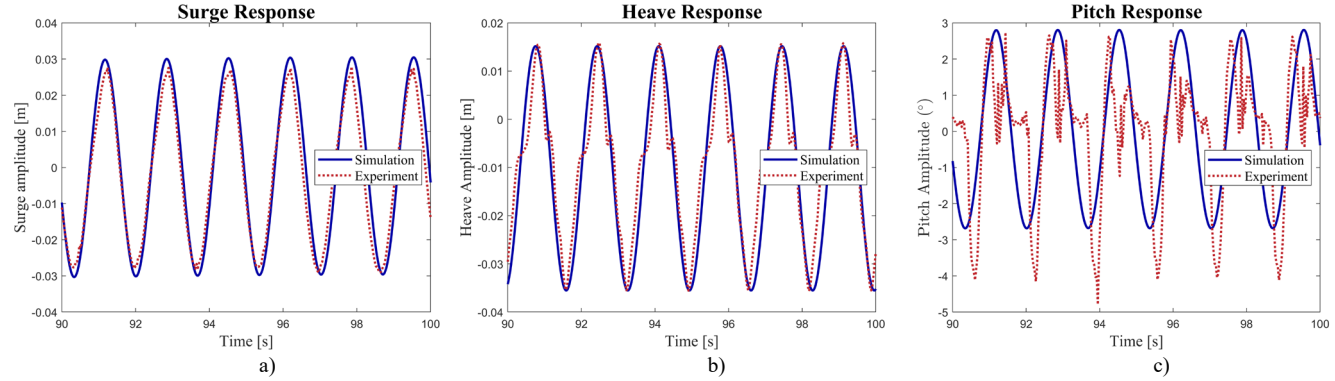

Fig. 6. Validation of the surge, heave, and pitch responses of the floater in the model through experiments within a 10-second timeframe (90-100 seconds) where steady conditions exist.

accuracy with some slight but acceptable discrepancies. However, the pitch motion presents a different behaviour. In the numerical model, the pitch motion exhibits smooth crests and troughs, creating a uniform and consistent signal. On the other hand, the experimental signal of the pitch motion has a different trend, characterized by discontinuous motion between the crest and the trough. These deviations can be attributed to the fact that the experimental conditions are considerably more complex and subjected to a variety of influencing factors that cannot be captured by the present numerical models, such as viscosity effects which are not accounted by the potential flow theory. Additionally, the actual mooring configuration could exhibit dynamic tensions which are difficult to model accurately.

Although these deviations are observed, it is demonstrated that the model's overall performance in replicating the surge and heave motions, which are of critical importance to the understanding of the floater's behaviour, is promising. With further refinements and more detailed modelling, the accuracy of the pitch motion prediction could be improved in a future work.

K. *Effects of the unstretched length on the response of the floater*

Following the validation of the numerical model with experimental measurements, the influence of the unstretched length of the mooring lines on the surge motion of the floater was investigated and the results are reported in this section. The heave and surge responses, mean position of the floater, and tension on the mooring lines were evaluated under different values of stiffness of the mooring lines and wave conditions. These interplaying parameters play a key role in fine-tuning the mooring lines, aiming to achieve the maximization of the surge amplitude.

9) *Influence of stiffness*

Fig. 7a presents the mean surge amplitude for varying unstretched lengths of the mooring cables, given different stiffness conditions. Each stiffness value corresponds to a different scenario of different rope material or diameter. Each data point on the graph represents a full 110 second simulation, with the unstretched length along the horizontal axis and the mean surge response along the vertical axis. Similarly, fig. 7b-d depict the mean heave amplitude, the mean position of the floater, and the mean peaks of mooring tensions, respectively, following the same format. These figures offer an expansive view of the

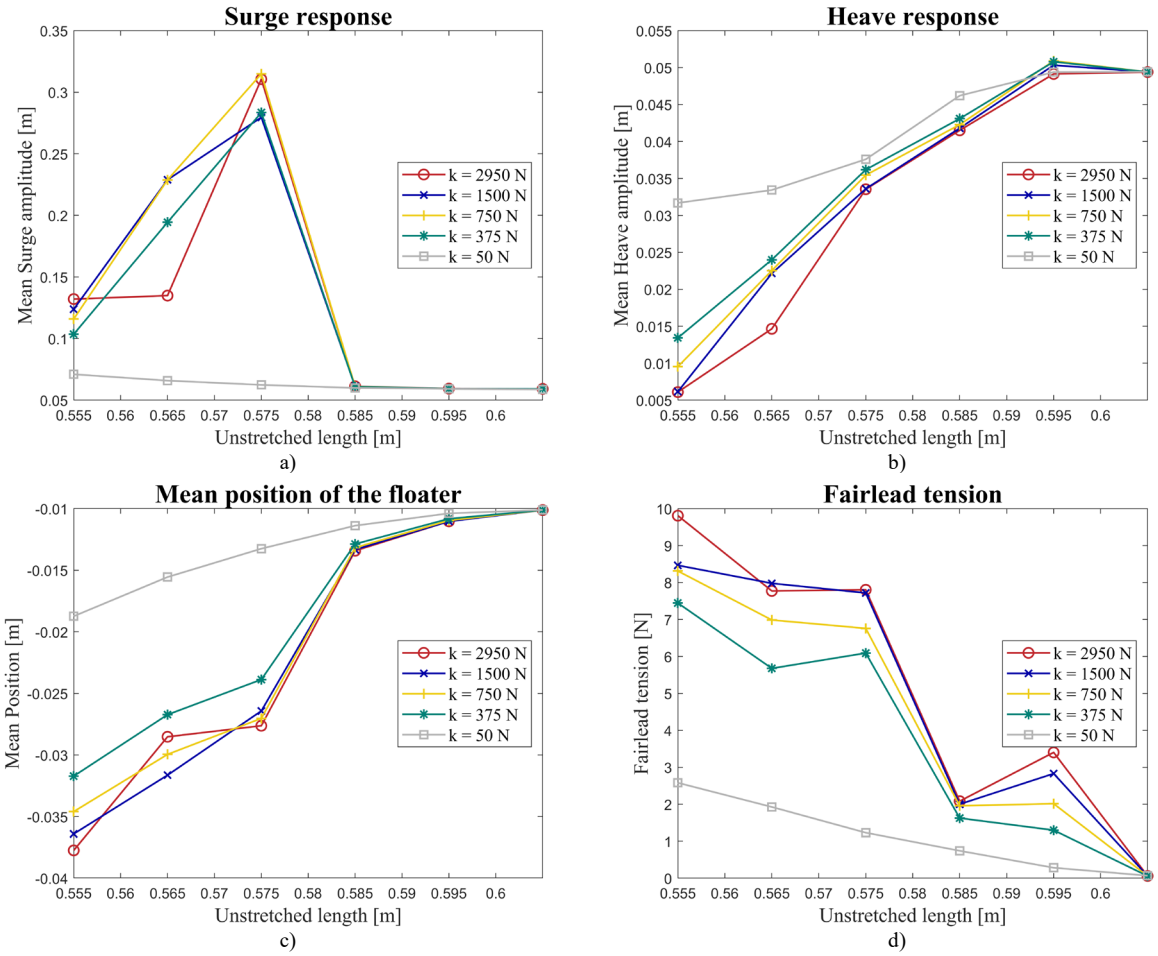

Fig. 7. Response of the mooring-floater system for different unstretched mooring line lengths and stiffness conditions: a) Mean surge amplitude, b) Mean heave amplitude, c) Mean position of the centre of gravity of the floater, d) Mean peaks on the mooring fairlead tensions. Each data point represents a full 110-second simulation.

relationships between the unstretched length, stiffness variations, and the respective responses, establishing a holistic understanding of the model behaviour under different conditions.

The results in fig. 7a demonstrate an interesting dynamical behaviour of the system in terms of the surge amplitude as the unstretched length is varied. For unstretched lengths larger than 0.585 m, the surge response exhibits minimal amplitude variations (in the range of 0.058 – 0.060 m), regardless of the stiffness. For shorter unstretched lengths (0.555 – 0.575 m), a significant increase in the surge response is observed. A peak is captured at an unstretched length of 0.575 m, for all cases except in the case with stiffness $k = 50\ N$. Further decrease in the unstretched length to 0.565 m and 0.555 m exhibits a descending surge response trend. This dynamical surge-response suggests that an optimum value exists for the unstretched length where the amplitude of surge motion can be maximized, providing a potential tuning parameter for enhancing wave energy capture in the surge direction.

However, the surge response behaviour should not be assessed in isolation, as it is closely linked to the responses in other degrees of freedom. Fig. 7b displays the mean heave amplitude as a function of the unstretched length across various stiffness conditions. Similar to the surge response, the heave response appears consistent for higher unstretched lengths (0.595 and 0.605 m). However, reducing the unstretched length causes a monotonic decline in the heave response. The inverse relationship between heave and surge response suggests a shift in energy distribution within the system.

The floater's mean position, represented by the position of its centre of gravity, is illustrated in fig. 7c. The graph shows a decrease of the mean position (i.e., increase of draft) with decreasing unstretched length, as expected. Moreover, an overall trend indicates that for a given unstretched length, higher stiffness values correspond to a lower floater position, suggesting an increased submerged depth of the floater for stiffer mooring lines.

Lastly, fig. 7d shows the mean peaks of mooring tensions on the fairlead (i.e., the component that connects the mooring lines to the floater), enabling us to understand the developed forces in the mooring line system under varying conditions, thereby completing our comprehensive understanding of the system's behaviour. It can be observed that the tensions in the mooring cables increase when the unstretched length decreases which was expected since the pre-tension is intensified by this change.

The inverse relationship between heave and surge response implies that energy initially transferred in the vertical direction of the waves (heave) shifts to the horizontal (surge) direction as the unstretched length

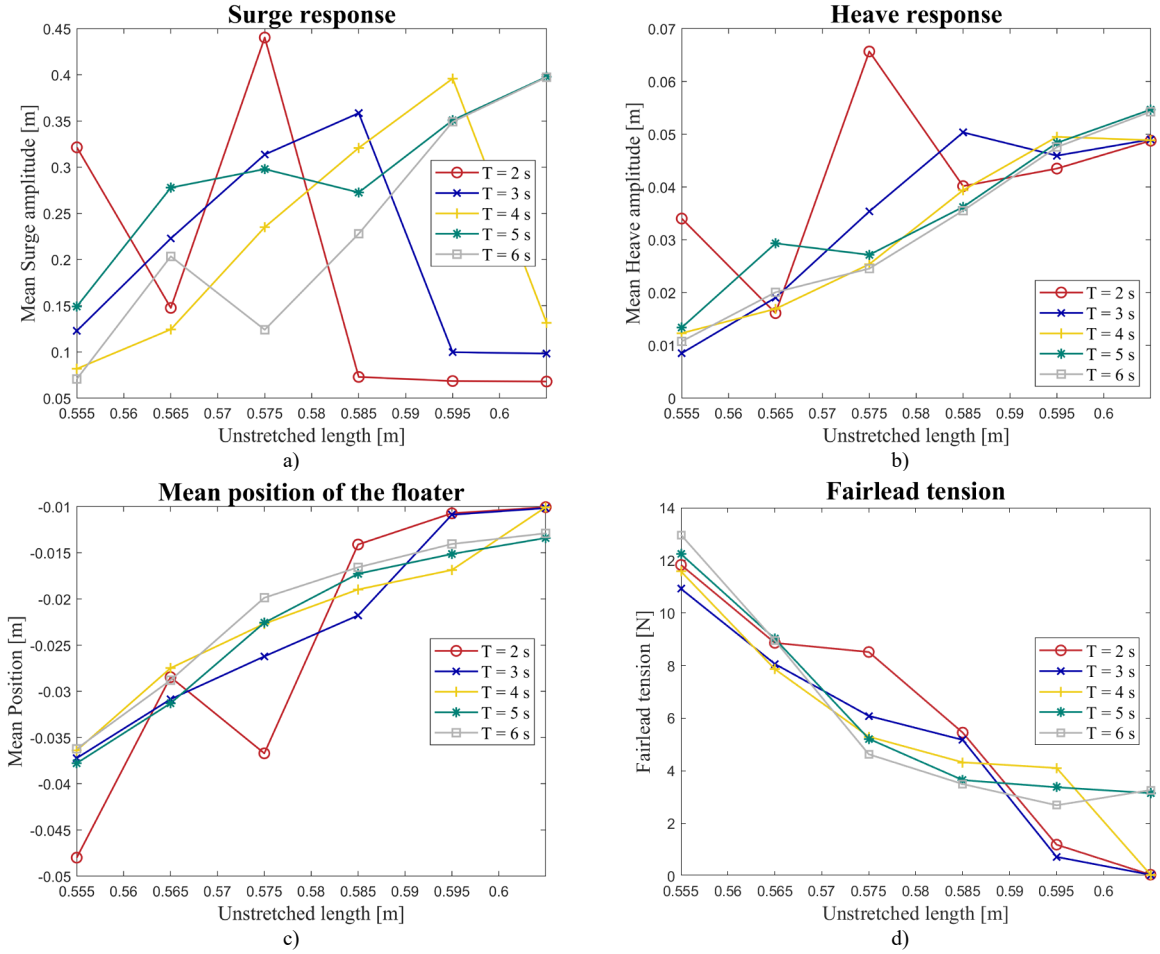

Fig. 8. Response of the mooring-floater system for various unstretched mooring line lengths under different wave conditions: a) Mean surge amplitude, b) Mean heave amplitude, c) Mean position of the centre of gravity of the floater, d) Mean peaks on the mooring fairlead tensions. Each data point represents a full 110-second simulation.

decreases. As the floater submerges deeper into the water due to a shorter unstretched length, the increase in the mooring force changes the dynamic behaviour of the floater, resulting in less energy being transferred in the vertical direction (heave) and more being redirected towards the horizontal direction (surge). With the decrease in the unstretched length, the wave energy, initially directed mostly to vertical oscillations, is gradually transferred to horizontal oscillations, hence underpinning the surge response enhancement seen in fig. 7a.

These results are of critical importance since they reveal the system's response to changes in mooring configuration. Furthermore, they provide evidence to exploit this adaptability of energy reallocation from vertical (heave) to horizontal (surge) movements. This study provides an advantageous adjustment parameter (i.e., the unstretched length) to fine-tune the system's performance for particular operational circumstances and energy extraction targets which in this case refer to future surge energy extraction mechanisms.

10) Influence of wave frequencies

This subsection presents an analysis of the influence of wave frequencies on the response of the floater and its mooring system. The considered frequencies range from 2 to 6 seconds in increments of 1 second. Throughout this analysis, the stiffness of the mooring lines is kept constant at the original numerical model's configuration value of $k = 2950\ N$. The aim of this study is to examine the varying effect of wave frequencies on the system's response and to assess how the optimum unstretched length value shifts across a spectrum of frequencies.

Fig. 8a presents the mean surge amplitude as a function of unstretched length across a range of wave periods. It is observed that each wave period corresponds to a different optimal value of the unstretched length that maximizes the surge amplitude. Specifically, for a wave period of T = 2 s, the optimum unstretched length is found to be 0.575 m. As the wave period increases to T = 3 s, this optimal value shifts to 0.585 m. Similarly, for T = 4 s, the optimal unstretched length is 0.595 m. Furthermore, for the larger wave periods tested (T = 5 s and T = 6 s), the optimal unstretched length was found to increase to 0.605 m.

This analysis highlights a clear trend suggesting that, as the wave period increases, the optimum value of the unstretched length also increases. This relationship was expected since the surge response of the floater depends on the wavelength. The understanding and quantification of this interplay between wave period and optimum unstretched length is crucial, since it allows for adjustments to the system's configuration based on the prevailing wave conditions, enabling maximization of surge response and, consequently, energy extraction from this motion.

The trends of the heave response, mean position of the floater and the tension on the fairlead demonstrate a similar behaviour to that of fig. 7. For lower values of unstretched length, the mean heave amplitude and the mean position of the floater decreases while the tension in the mooring lines increases.

However, an interesting observation emerges when considering the wave period of $T = 2\ s$, specifically at an unstretched length of $0.575\ m$. Contrary to expectation, both the surge and heave amplitudes exhibit a simultaneous increase. Typically, it would be anticipated that an enhanced surge response would be accompanied by a reduced heave response, due to the energy reallocation from the vertical to the horizontal direction as analysed earlier. This observation suggests that there is a more complex interaction between the floater and the waves at this specific configuration. At the same time, the mean position of the floater shows a notable decrease, indicating an increase in the floater's draft. The submergence of the floater influences the hydrodynamic forces acting on it and changes the nature of its interaction with the incident waves. This could potentially explain the synchronous rise in both surge and heave responses. The collective surge-heave behaviour observed at this unique configuration signifies that the energy redistribution from heave to surge is not always straightforward and can be influenced by other factors such as the depth of submergence and the wave characteristics.

This finding highlights the significance of investigating and understanding these complex interactions to optimize the system's response under varying wave conditions and mooring configurations.

V. Conclusions and Future Work

In this study a series of numerical and experimental tests were performed to analyse the motion of a moored floater. The numerical tests were conducted with a coupled numerical model of WEC-Sim and MoorDyn which was validated against the experiments. The model replicated the response of an actual moored cuboid floater with reasonable accuracy. The analysis outlined the pivotal role of the unstretched length of the mooring cable, revealing its potential as a tuning parameter for enhancing the surge response of the floater under varying stiffness values and wave conditions. Through a detailed analysis, it was demonstrated that an optimal value of the unstretched length for the mooring line exists, which ensures maximum surge amplitude under a variety of conditions.

This research lays the foundations for designing wave energy converters that could harness energy from both the heave and surge motions, through strategic adjustment of the taut mooring configuration. Prospective research could extend to testing the model under irregular waves and developing a control strategy to control the unstretched length in real-time, optimising energy extraction efficiency in line with variable wave conditions. In conclusion, this study paves a promising trajectory for more sophisticated and adaptive wave energy conversion mechanisms.

VI. References

[1] T. Aderinto and H. Li, "Review on Power Performance and Efficiency of Wave," *Energies,* vol. 12, no. 22, 2019.

[2] B. Guo, T. Wang, S. Jin, S. Duan, K. Yang and Y. Zhao, "A Review of Point Absorber Wave Energy Converters," *Journal of Marine Science and Engineering,* vol. 10, no. 10, 2022.

[3] C. S.-W. Kester Gunn, "Quantifying the global wave power resource," *Renewable Energy,* vol. 44, pp. 296-304, 2012.

[4] D. Qiao, R. Haider, J. Yan, D. Ning and B. Li, "Review of Wave Energy Converter and Design of Mooring System," *Sustainability,* vol. 12, no. 19, 2020.

[5] E. Lejerskog, H. Gravråkmo, A. Savin, E. Strömstedt, S. Tyrberg, K. Haikonen, R. Krishna, C. Boström, M. Rahm, R. Ekström, O. Svensson, J. Engström, B. Ekergård, A. Baudoin, V. Kurupath, L. Hai, W. Li, J. Sundberg, R. Waters and M. Leijon, "Lysekil Research Site, Sweden: A Status Update," in *9th European Wave and Tidal Energy Conference (EWTEC 2011)*, Southampton, 2011.

[6] M. H. Jahangir and S. G. Motlagh, "Feasibility study of CETO wave energy converter in Iranian coastal areas to meet electrical demands (a case study)," *Energy for Sustainable Development,* vol. 70, pp. 272-289, 2022.

[7] E. Amini, R. Asadi, D. Golbaz, M. Nasiri, S. T. O. Naeeni, M. M. Nezhad, G. Piras and M. Neshat, "Comparative Study of Oscillating SurgeWave Energy Converter Performance: A Case Study for Southern Coasts of the Caspian Sea," *Sustainability,* vol. 13, no. 10932, 2021.

[8] A. Garcia-Teruel and D. Forehand, "A review of geometry optimisation of wave energy converters," *Renewable and Sustainable Energy Reviews,* vol. 139, no. 110593, 2021.

[9] E. Amini, H. Mehdipour, E. Faraggiana, D. Golbaz, S. Mozaffari, G. Bracco and M. Neshat, "Optimization of hydraulic power take-off system settings for point absorber wave energy converter," *Renewable Energy,* vol. 194, pp. 938-954, 2022.

[10] R. Alamian, R. Shafaghat and M. R. Safaei, "Multi-Objective Optimization of a Pitch Point Absorber Wave Energy Converter," *Water,* vol. 11, no. 5, 2019.

[11] H. Shi, Z. Han and C. Zhao, "Numerical study on the optimization design of the conical bottom heaving buoy convertor," *Ocean Engineering,* vol. 173, pp. 235-243, 2019.

[12] T. D. Dang, C. B. Phan and K. K. Ahn, "Design and Investigation of a Novel Point Absorber on Performance Optimization Mechanism for Wave Energy Converter in Heave Mode," *International Journal of Precision Engineering and Manufacturing-Green Technology,* vol. 6, p. 477–488, 2019.

[13] I. A. Ja'e, M. O. A. Ali, A. Yenduri, Z. Nizamani and A. Nakayama, "Optimisation of mooring line parameters for offshore floating structures: A review paper," *Ocean Engineering,* vol. 247, no. 110644, 2022.

[14] S. Wilson, M. Hall, S. Housner and S. Sirnivas, "Linearized modeling and optimization of shared mooring systems," *Ocean Engineering,* vol. 241, no. 110009, 2021.

[15] G. Ferri, E. Marino, N. Bruschi and C. Borri, "Platform and mooring system optimization of a 10 MW semisubmersible offshore wind turbine," *Renewable Energy,* vol. 182, pp. 1152-1170, 2022.

[16] W. E. Cummins, "THE IMPULSE RESPONSE FUNCTION AND SHIP MOTIONS," in *SYMPOSIUM ON SHIP TREORY*, Hamburg, 1962.

[17] D. Ogden, K. Ruehl, Y.-H. Yu, A. Keester, D. Forbush, J. Leon and N. Tom, "Review of WEC-Sim Development and Applications," *INTERNATIONAL MARINE ENERGY JOURNAL,* vol. 5, no. 3, 2022.

[18] C. Windt, J. Davidson and J. V. Ringwood, "High-fidelity numerical modelling of ocean wave energy systems: A review of computational fluid dynamics-based numerical wave tanks," *Renewable and Sustainable Energy Reviews,* vol. 93, pp. 610-630, 2018.

[19] J. Palm, C. Eskilsson, G. M. Paredes and L. Bergdahl, "Coupled mooring analysis for floating wave energy converters using CFD: Formulation and validation," *International Journal of Marine Energy,* vol. 16, pp. 83-99, 2016.

[20] B. Devolder, V. Stratigaki, P. Troch and P. Rauwoens, "CFD Simulations of Floating Point Absorber Wave Energy Converter Arrays Subjected to Regular Waves," *Energies,* vol. 11, no. 641, 2018.

[21] F. Pierart, J. Fernandez, J. Olivos, R. Gabl and T. Davey, "Numerical Investigation of the Scaling Effects for a Point Absorber," *Water,* vol. 14, no. 2156, 2022.

[22] M. A. Bhinder, C. G. Mingham, D. M. Causon, M. T. Rahmati, G. A. Aggidis and R. V. Chaplin, "A Joint Numerical and Experimental Study of a Surging Point Absorbing Wave Energy Converter (WRASPA)," in *28th International Conference on Ocean, Offshore and Arctic Engineering*, Honolulu, 2010.

[23] K. Ruehl, D. Ogden, Y.-H. Yu, A. Keester, N. Tom, D. Forbush, J. Leon, J. Grasberger and S. Husain, "WEC-Sim," National Renewable Energy Laboratory and National Technology & Engineering Solutions of Sandia, LLC (NTESS), 2023. [Online]. Available: https://wec-sim.github.io/WEC-Sim/master/theory/index.html. [Accessed May 2023].

[24] M. Ancellin, "Capytaine: a Python-based distribution of Nemoh," 2022. [Online]. Available: https://ancell.in/capytaine/latest/. [Accessed May 2023].

[25] M. Hall, "MoorDyn," 2023. [Online]. Available: http://www.matt-hall.ca/moordyn.html. [Accessed May 2023].

[26] S. Sirnivas, Y.-H. Yu, M. Hall and B. Bosma, "COUPLED MOORING ANALYSES FOR THE WEC-SIM WAVE ENERGY CONVERTER DESIGN TOOL," in *Proceedings of the ASME 2016 35th International Conference on Ocean, Offshore and Arctic Engineering*, Busan, 2016.

[27] F. F. Wendt, M. T. Andersen, A. N. Robertson and J. M. Jonkman, "Verification and Validation of the New Dynamic Mooring Modules Available in FAST v8," in *26th International Ocean and Polar Engineering Conference*, Rhodes, 2016.

[28] H. Chen and M. Hall, "CFD simulation of floating body motion with mooring dynamics: Coupling MoorDyn with OpenFOAM," *Applied Ocean Research,* vol. 124, no. 103210, 2022.

[29] R. Verma, "AN EFFICIENT COLOR-BASED OBJECT DETECTION AND TRACKING IN VIDEOS," *International Journal of Computer Engineering and Applications,* vol. XI, no. XI, 2017.

[30] H. G. Limited, Marine Equipment and Wire Rope Handbook, HER Group, 1990.